Journal of Hazardous Materials 386 (2020) 121970

Contents lists available at ScienceDirect

Journal of Hazardous Materials

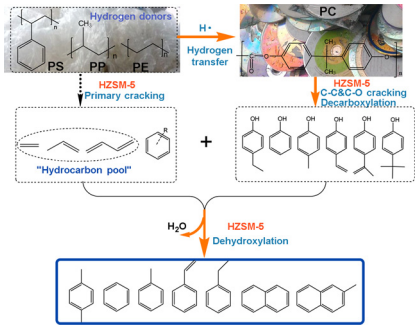
journal homepage: www.elsevier.com/locate/jhazmat

Converting polycarbonate and polystyrene plastic wastes intoaromatic hydrocarbons via catalytic fast co-pyrolysis

Jia Wang[a,b,c,d], Jianchun Jiang[a,b,*], Xiaobo Wang[e], Ruizhen Wang[a,b], Kui Wang[a,b], Shusheng Pang[f], Zhaoping Zhong[c], Yunjuan Sun[b,**], Roger Ruan[g], Arthur J. Ragauskas[d,h,i]

[a] Jiangsu Co-Innovation Center of Efficient Processing and Utilization of Forest Resources, College of Chemical Engineering, Nanjing Forestry University, Longpan Road 159, Nanjing 210037, China
[b] Institute of Chemical Industry of Forest Products, Chinese Academy of Forestry (CAF), No. 16, Suojin Five Village, Nanjing, Jiangsu 210042, China
[c] Key Laboratory of Energy Thermal Conversion and Control of Ministry of Education, Southeast University, No.2 Sipailou, Xuanwu District, Nanjing, Jiangsu 210096, China
[d] Department of Chemical & Biomolarcular Engineering, the University of Tennessee, Knoxville, TN 37996, USA
[e] School of Environmental Science, Nanjing Xiaozhuang University, Nanjing, Jiangsu 211171, China
[f] Department of Chemical and Process Engineering, University of Canterbury, Christchurch, New Zealand
[g] Center for Biorefining and Department of Bioproducts and Biosystems Engineering, University of Minnesota, 1390 Eckles Ave., St. Paul, MN 55108, USA
[h] Department of Forestry, Wildlife and Fisheries, Center for Renewable Carbon, the University of Tennessee, Institute of Agriculture, Knoxville, TN 37996, USA
[i] Joint Institute for Biological Science, Biosciences Division, Oak Ridge National Laboratory, Oak Ridge, TN 37831, USA

GRAPHICAL ABSTRACT



ARTICLE INFO

Editor: R. Teresa

Keywords:
Plastic polymers
Bisphenol A polycarbonate
Catalytic thermochemical conversion
HZSM-5
Monocyclic aromatic hydrocarbons

ABSTRACT

Thermochemical conversion of plastic wastes is a promising approach to produce alternative energy-based fuels. Herein, we conducted catalytic fast co-pyrolysis of polycarbonate (PC) and polystyrene (PS) to generate aromatic hydrocarbons using HZSM-5 (Zeolite Socony Mobil-5, hydrogen, Aluminosilicate) as a catalyst. The results indicated that employing HZSM-5 in the catalytic conversion of PC facilitated the synthesis of aromatic hydrocarbons in comparison to the non-catalytic run. A competitive reaction between aromatic hydrocarbons and aromatic oxygenates was observed within the studied temperature region, and catalytic degradation temperature of 700 °C maximized the competing reaction towards the formation of targeted aromatic hydrocarbons at the expense of phenolic products. Catalyst type also played a vital role in the catalytic decomposition of PC wastes,

* Corresponding author at: Jiangsu Co-Innovation Center of Efficient Processing and Utilization of Forest Resources, College of Chemical Engineering, Nanjing Forestry University, Longpan Road 159, Nanjing 210037, China.
** Corresponding author at: Institute of Chemical Industry of Forest Products, Chinese Academy of Forestry (CAF), No. 16, Suojin Five Village, Nanjing, Jiangsu 210042, China.
E-mail addresses: jiangjc@icifp.cn (J. Jiang), bioenergy@seu.edu.cn (Y. Sun).

https://doi.org/10.1016/j.jhazmat.2019.121970
Received 2 October 2019; Received in revised form 21 December 2019; Accepted 23 December 2019
Available online 24 December 2019
0304-3894/ © 2019 Elsevier B.V. All rights reserved.

and HZSM-5 with different Si/Al molar ratios produced more aromatic hydrocarbons than HY (Zeolite Y, hydrogen, Faujasite). Regarding the effect of Si/Al molar ration in HZSM-5 on the distribution of monocyclic aromatic hydrocarbons (MAHs), a Si/Al molar ratio of 38 maximized benzene formation with an advanced factor of 5.1. Catalytic fast co-pyrolysis of PC with hydrogen-rich plastic wastes including polypropylene (PP), polyethylene (PE), and polystyrene (PS) favored the production of MAHs, and PS was the most effective hydrogen donor with a ~2.5-fold increase. The additive effect of MAHs increased at first and then decreased when the PC percentage was elevated from 30 % to 90 %, achieving the maximum value of 32.4 % at 70 % PC.

1. Introduction

Bisphenol A polycarbonate (PC) is a leading engineering plastic due to its excellent chemical and physical properties, including good thermal stability and ductility, excellent transparency, and high mechanical strength (Tang et al., 2019; Antonakou et al., 2014a; Antonakou and Achilias, 2012). Therefore, PC has been extensively employed in electrical and electronic appliances and automotive industry, with an annual production of ~6 million tons (Do et al., 2018). However, the massive employment of PC polymers has resulted in an abundance of PC wastes that need to be disposed of. Conventional waste management methods for plastic wastes such as incineration and/or landfill are not suitable for PC wastes, as these processes lead to the release of bisphenol A (an endocrine disruptor) which is potentially harmful to both humans and environment (Antonakou et al., 2014b). Hence, more efforts are still needed in exploring environmentally friendly and cost-efficient approaches to effectively dispose of PC wastes.

Among the recycling methods to treat plastic wastes, the thermochemical conversion of plastic polymers into alternative energy-based resources has received considerable attention (Yao et al., 2018a; Shahid et al., 2019). Typically, fast pyrolysis (FP) which is conducted in the absence of oxygen at moderate temperature, targeting at the production of value-added chemicals and/or fuel additives, has been recognized as a meaningful utilization approach (Yao et al., 2018b; Mehmood et al., 2019). However, one of the drawbacks of FP is the wide distribution of pyrolytic compounds and low content of specific targets such as aromatic hydrocarbons. Thus, employing suitable catalysts in the FP (i.e., catalytic fast pyrolysis, CFP) is beneficial to the thermochemical decomposition of plastics by tailoring product composition (Xue and Bai, 2018; Zhang et al., 2019a). It's noteworthy that acidic zeolites with strong acidity and distinct pore structure, such as HZSM-5 (Zeolite Socony Mobil-5, hydrogen, Aluminosilicate) and HY (Zeolite Y, hydrogen, Faujasite), have been proven as effective catalysts which facilitate the C—C bond scission and the formation of aromatic hydrocarbons (Sebestyén et al., 2017; Park et al., 2019a). Moreover, aromatic hydrocarbons, in particular for monocyclic ones including benzene, toluene, and xylene, are basic organic chemicals with great market demand (Zhang et al., 2018). For instance, toluene can be blended into gasoline because of its high octane number or utilized as a feedstock to produce polyurethanes (Zhang et al., 2019b). In this regard, catalytic conversion of PC over acidic zeolites to generate aromatic hydrocarbons could be a promising way to dispose of plastic wastes.

Although employing catalysts in the catalytic conversion of PC is beneficial to form aromatic hydrocarbons, the high oxygen content and low H/C effective ratio of PC also limited the generation of desirable aromatic products. Zhang et al. (2011) reported that elevating the H/C effective ratio in feedstocks promoted the formation of olefins and aromatics in the catalytic fast pyrolysis of biomass-derived samples, and a high H/C effective ratio of feedstocks also boosted the stability of HZSM-5 by mitigating coke accumulation. Therefore, hydrogen-rich waste plastic polymers, including polypropylene (PP) and polyethylene (PE), were extensively used as hydrogen donors in the co-pyrolysis of biomass to enhance the production of aromatic hydrocarbons (Park et al., 2018; Rezaei et al., 2017; Wang et al., 2019). For instance, Ryu et al., (2019) conducted the co-pyrolysis of cellulose and LLDPE (linear low-density polyethylene, LLDPE) over MgO-impregnated catalysts, and it was observed that LLDPE co-fed with cellulose produced more aromatic hydrocarbons. However, to the best of our knowledge, co-feeding PC with hydrogen-rich plastics such as PE, PP, and polystyrene (PS) to improve the H/C effective ratio of feedstocks, in particular with an emphasis on advanced generation of monocyclic aromatic hydrocarbons (MAHs), has not been reported yet.

In the present study, catalytic fast co-pyrolysis of PC with hydrogen-rich plastics over HZSM-5 or HY was conducted. The effect of reaction temperature on catalytic degradation of PC wastes and the distribution of pyrolytic volatile matters was explored at first. Subsequently, the influence of catalyst type and Si/Al molar ratio in HZSM-5 on the formation of aromatic hydrocarbons were investigated to screen suitable catalysts in the catalytic conversion of PC. Thirdly, hydrogen-rich plastic wastes including PP, PE, and PS, were employed to co-pyrolyze with PC for improved production of targeted aromatic hydrocarbons, and the optimal hydrogen donor was screened. Finally, the additive effect between PC and PS during the co-pyrolysis process was thoroughly studied to maximize the formation of MAHs.

2. Experimental

2.1. Materials

Powdered polymer plastics (~0.15 mm), which include PE, PS, PP, and PC, were obtained from Huachuang Polymer Materials Company in Guangdong province, China. The elemental analysis of plastic samples was conducted, and the results are shown in Table S1. HY and HZSM-5 (Si/Al molar ratio: 25, 38, and 50), were provided by the Catalyst Plant of Nankai University, Tianjin, China, and they were used as received.

2.2. Experimental method

Catalytic and non-catalytic degradation of plastic wastes were performed by an analytical micro pyrolyzer (5200, CDS Analytical, USA) connected with a gas chromatography/mass spectrometry (GC/MS, 7890A/5975C, Agilent). The plastic samples (~1 mg) and catalysts (~1.5 mg) were loaded in a quartz tube that was 20 mm in length and 2 mm in diameter, and the schematic diagram of the quartz tube is shown in Fig. S1. The heating rate was kept at 20 °C/ms and the retention time was 15 s, and analytical high purity helium (99.999 %) was used as the carrier gas. The NIST MS library database was employed to identify the pyrolytic volatile matters, and the content of pyrolytic vapors was determined by the peak area of the total ion current (TIC) chromatogram, which is the same methodology as reported by Zhang et al. (2019c) and Kassargy et al. (2019). Moreover, each experiment was repeated at least twice to ensure reproducibility.

The relative selectivity of aromatic hydrocarbons or phenolic products (S_{ap}) was calculated based on related studies (Zhang et al., 2017a, b), shown as below:

$$S_{ap} = \frac{P_s}{\sum P_{ap}} \quad (1)$$

where P_s and ΣP_{ap} are the peak area of specific products and the total peak area of aromatic hydrocarbons or phenols, respectively.

To evaluate the performance of studied catalysts in the catalytic

conversion of plastic wastes, the advanced factor (A_f) of MAHs was calculated, shown as follows:

$$A_f = \frac{p_{s(i)} - p_{c(i)}}{p_{c(i)}} \quad (2)$$

where $p_{c(i)}$ is the TIC area of specific MAHs obtained from the non-catalytic trial, $p_{s(i)}$ is the TIC area of specific MAHs obtained from catalytic conversion of plastic wastes over HY or HZSM-5 with different Si/Al molar ratios.

3. Results and discussion

3.1. Optimization of reaction temperature

It is well known that catalyst is crucial to catalytic degradation of plastics since it tailors product distribution and improves the quality of pyrolytic vapors by selectively producing more desirable fractions. In this work, a comparative study of non-catalytic and catalytic fast pyrolysis of PC was conducted at first, with an emphasis on exploring the effect of catalyst on the production of aromatic hydrocarbons. The reaction temperature was kept at 700 °C, and HZSM-5 with a Si/Al molar ratio of 38 was employed as a catalyst. Fig. 1 shows the GC/MS chromatograms of pyrolytic products derived from both non-catalytic and catalytic conversion of PC polymers (pyrolytic products derived from non-catalytic as a function of reaction temperature shown in Fig. S2). Typically, thermochemical decomposition of PC produced a series of aromatic compounds including aromatic hydrocarbons (such as benzene, toluene, and naphthalene) and phenolic products such as phenol and cresols. As expected, compared to the non-catalytic trial, an introduction of HZSM-5 (38) in the catalytic degradation of PC considerably produced more aromatic hydrocarbons with a ~5-fold increase, while the phenolic products were dramatically inhibited. Generally, the presence of acidic catalysts with Brønsted acid sites promoted the formation of H^+ attack oligomers, which further facilitated the production of aromatic hydrocarbons by cracking (C-C and C-O breaking), dehydration, decarboxylation, decarbonylation, dealkoxylation, and aromatization (Bai et al., 2019; Mullen and Boateng, 2010; Ben and Ragauskas, 2013). Besides, pyrolytic gas products (CO& CO_2) were accelerated in the presence of HZSM-5, indicating deoxygenation reactions such as decarbonylation and decarboxylation were enhanced. Therefore, introducing HZSM-5 facilitated the degradation of PC and improved the quality of pyrolytic volatile matters by forming more targeted aromatic hydrocarbons.

1. CO&CO_2; 2. benzene; 3. toluene; 4. ethylbenzene; 5. *p*-xylene; 6. penylethyne; 7. styrene; 8. phenol; 9. benzene, 1-propynyl-; 10. cresol; 11. naphthalene; 12. naphthalene, 1-methyl-; 13. naphthalene, 2-methyl-; 14. *p*-iso propenylphenol; 15. biphenyl; 16. biphenylene; 17. fluorene.

Fig. 2 illustrates the pyrolytic products derived from catalytic fast pyrolysis of PC over HZSM-5 as a function of reaction temperature (ranging from 600 °C to 800 °C with a temperature interval of 50 °C). As indicated, catalytic degradation temperature played a determining role in the conversion of PC polymers as a competitive reaction between aromatic hydrocarbons and aromatic oxygenates was observed within the studied temperature region. More specifically, there was a significant increase in aromatic hydrocarbons when elevating the reaction temperature from 600 °C to 700 °C, while further increasing the temperature to 800 °C suppressed the formation. Conversely, aromatic oxygenates decreased at first and then slightly increased with the lowest obtained at 700 °C. Hence, a catalytic degradation temperature of 700 °C maximized the competitive reaction towards the generation of aromatic hydrocarbons at the expense of phenolic products.

Moreover, the distribution of aromatic hydrocarbons and oxygenates are also illustrated in Fig. 2. The aromatic hydrocarbons comprised of MAHs (such as benzene, toluene, ethylbenzene, xylenes, and styrene) and BAHs (bicyclic aromatic hydrocarbons, dominated by naphthalene and its derivates), and the pyrolytic aromatic oxygenates mainly were phenols, benzofurans, and negligible esters. As indicated, MAHs tended to increase at first and then decreased with the highest content achieving at 700 °C, and a similar trend was observed for BAHs. Concerning phenolic compounds produced in the catalytic conversion of PC over HZSM-5, elevating reaction temperature from 600 °C to 700 °C resulted in a prominent decrease, however, further increasing the reaction temperature to 800 °C slightly promoted the generation. Regarding benzofurans and esters, the content increased at first and then decreased with the highest value obtained at 700 °C. Overall, since aromatic hydrocarbons were desired products, and a reaction temperature of 700 °C maximized their production, therefore, the catalytic temperature was fixed at 700 °C.

3.2. Effect of catalyst type and Si/Al molar ratio in HZSM-5

During the catalytic conversion of plastic wastes, catalyst type and Si/Al molar ratio of HZSM-5 are also of importance to produce desirable aromatic hydrocarbons. In order to study the effect of catalyst type and Si/Al molar ratio of HZSM-5 on the generation of aromatic hydrocarbons in the catalytic fast pyrolysis of PC, catalysts including HY (Faujasite) and HZSM-5 (Aluminosilicate) with different Si/Al ratios (25, 38, and 50) were used, and the experimental results are presented in Fig. 3. As shown, compared to HY, HZSM-5 with varying Si/Al molar ratios were more active in producing aromatic hydrocarbons (both MAHs and BAHs), for instance, the total aromatic hydrocarbons obtained from HZSM-5 (38) catalyzed run was 1.6-fold greater than that achieved from the HY catalyzed trial. This might be attributed to the shape selectivity of HZSM-5 which led to the production of aromatic hydrocarbons. Specifically, compared to HY, the pore size of HZSM-5 (ca. 5.6 Å *vs.* ca. 7.6 Å for HY) is similar to the kinetic diameters of aromatic hydrocarbons (5.85 Å for benzene, toluene, and *p*-xylene), suggesting that HZSM-5 is more effective to produce MAHs (Jae et al., 2011). However, regarding the pyrolytic aromatic oxygenates, HY and HZSM-5 (50) produced comparable aromatic oxygenates (Fig. 3d), while HZSM-5 (25) and HZSM-5 (38) suppressed the generation with the lowest content attained at HZSM-5 (25). More specifically, phenols were enhanced with the elevating of the Si/Al molar ratio in HZSM-5. While for the benzofurans and esters, HZSM-5 (38) was more beneficial to their production.

To further investigate the effect of catalyst type and Si/Al molar ratio in HZSM-5 on the production of MAHs, Fig. 4 shows the distribution and advanced factor of main MAHs attained from catalytic fast pyrolysis of PC wastes. As observed, the distribution of MAHs was dominated by benzene and toluene, and HZSM-5 (38) maximized benzene formation with an advanced factor of 5.1 followed by HZSM-5

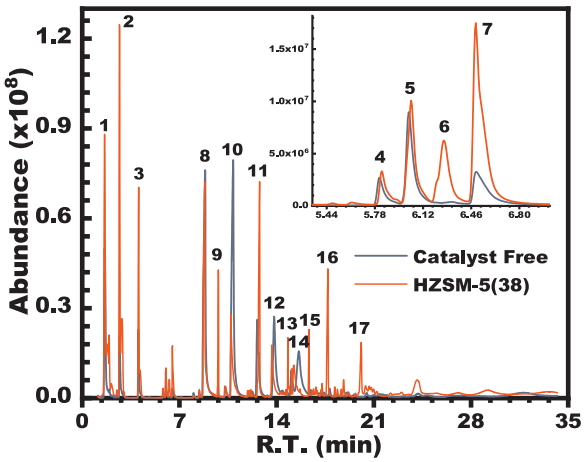


Fig. 1. GC/MS chromatograms derived non-catalytic and catalytic fast pyrolysis of PC over HZSM-5: Reaction temperature: 700 °C; Si/Al molar ratio: 38.

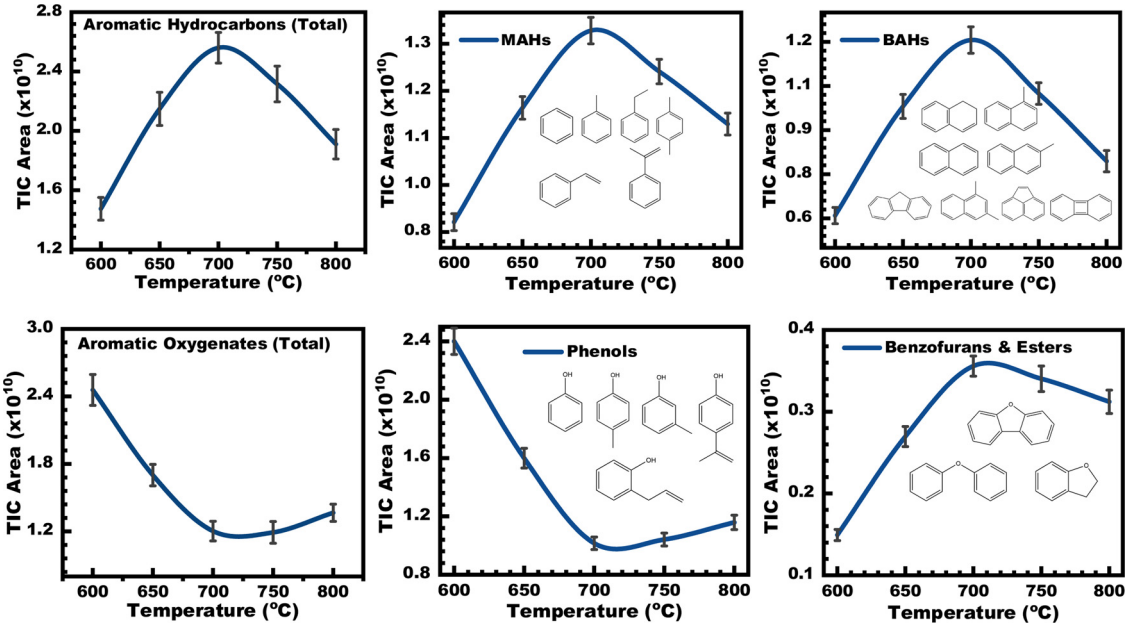


Fig. 2. Pyrolytic products obtained from catalytic fast pyrolysis of PC over HZSM-5(38).

(25) with a value of 4.0. A similar trend was observed for toluene and styrene as the advanced factors were increased to 1.95 and 2.7 in the presence of HZSM-5 (38), respectively. Conversely, HZSM-5 (38) was less effective to generate ethylbenzene and *p*-xylene as the advanced factors decreased at first and then increased within the studied Si/Al molar ratio range. Given HZSM-5 (38) was more effective to form both MAHs and BAHs, hence, it was screened for catalytic degradation of PC wastes.

3.3. Catalytic co-pyrolysis of PC with hydrogen-rich plastic wastes

As mentioned, the H/C effective ratio of feedstocks plays a vital role in generating aromatic hydrocarbons. Our previous work indicated that catalytic fast co-pyrolysis of biomass with hydrogen-rich plastic wastes enhanced the production of aromatic hydrocarbons (Wang et al., 2019). Therefore, to improve the H/C effective ratio of feedstocks (0.50 for PC, Table S1) for producing more MAHs, plastics including PE, PP, and PS were used as hydrogen donors (H/C effective ratios shown in Table S1) to co-feed with PC (mass ratio: 1:1) over HZSM-5 (38), and the experimental results are presented in Fig. 5. As observed, compared to catalytic conversion of pure PC, catalytic fast co-pyrolysis of PC with hydrogen-rich plastics facilitated the generation of MAHs at different levels. In a typical co-pyrolysis of PC and hydrogen-rich plastics over the HZSM-5 run, the PC-derived phenolic products are stabilized either by abstracting hydrogen atoms from plastic-derived alkanes or by accepting hydrogen atoms released from the aromatization of alkenes (Yu et al., 2019). Subsequently, the stabilized simple phenolic compounds and light olefins (known as “hydrocarbon pool”) originated from

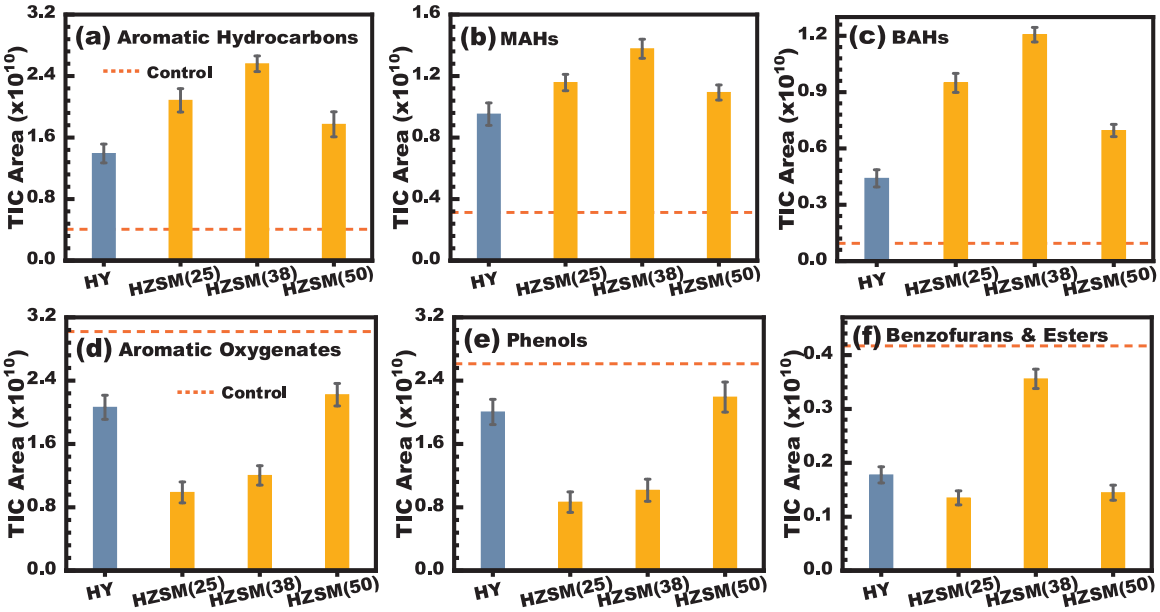


Fig. 3. Pyrolytic products obtained from catalytic fast pyrolysis of PC wastes over HY and HZSM-5: Effect of catalyst type and Si/Al molar ratio in HZSM-5; Red dashed line: control derived from non-catalytic run; HZSM-5 with Si/Al molar ratios of 25, 38, and 50 were labeled as HZSM-5(25), HZSM-5(38), and HZSM-5(30), respectively. (For interpretation of the references to colour in this figure legend, the reader is referred to the web version of this article).

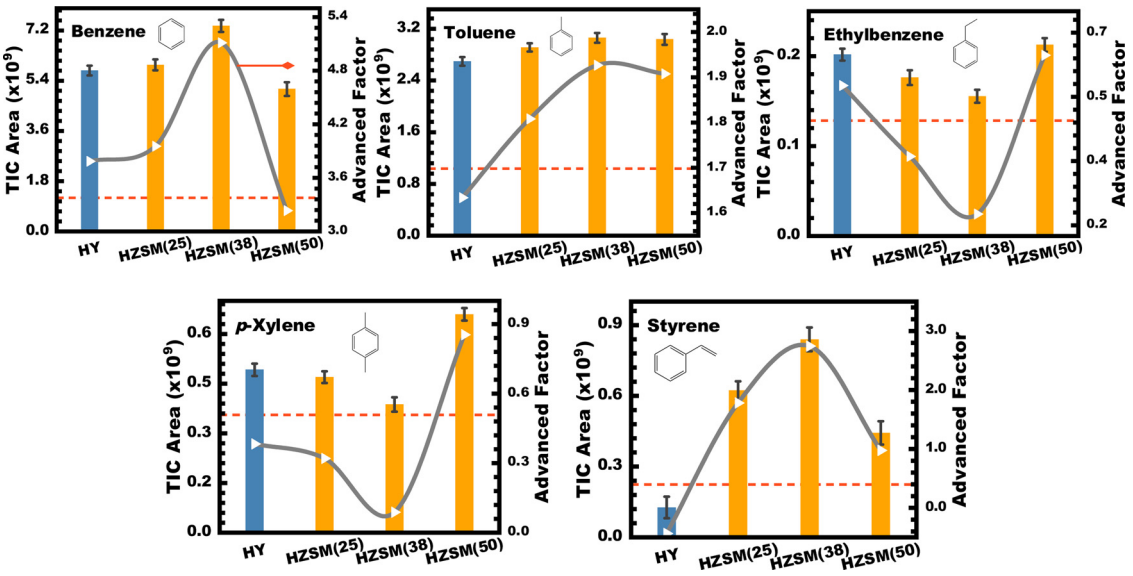


Fig. 4. Distribution and advanced factor of MAHs obtained from catalytic conversion of PC over HY and HZSM-5 with varying Si/Al molar ratios; Red dashed line: control derived from the non-catalytic run. HZSM-5 with Si/Al molar ratios of 25, 38, and 50 were labeled as HZSM-5(25), HZSM-5(38), and HZSM-5(30), respectively. (For interpretation of the references to colour in this figure legend, the reader is referred to the web version of this article).

primary cracking of hydrogen donors enter into the catalyst pores together to produce aromatic hydrocarbons via dihydroxylation, Diels-Alder cyclization, and aromatization reactions in the presence of HZSM-5 as shown in Scheme 1 (Park et al., 2019b; Zhang et al., 2016).

Among the hydrogen donors, PS was the most effective as a ~2.5-fold increase in MAHs was produced (GC/MS chromatograms shown in Fig. 6). Table 1 shows the detailed distribution of MAHs obtained from catalytic fast pyrolysis of pure PC, PS, and co-pyrolysis of PC with PS. As indicated, MAHs were significantly promoted upon using PS to co-pyrolyze with PC in comparison to those obtained from catalytic degradation of pure PC or PS. For example, benzene and toluene increased from 18.7 % and 9.7 % for pure PS to 26.3 % and 13.7 % in the co-pyrolysis run, respectively. Of particular interest was that the total MAHs reached 76.6 % in the catalytic fast co-pyrolysis run as opposed to 63.8 % and 22.6 % for catalytic conversion of pure PS and PC, respectively. Bai et al. (2019) also reached a similar conclusion who studied the depolymerization of high impact polystyrene (HIPS) using supercritical water, and it was observed that hydrogenation and demethylation are responsible for the production of stable MAHs such as toluene and ethylbenzene at a high reaction temperature.

Moreover, the theoretical MAHs which were calculated by linear superposition of individual feedstock with the assumption of no interactions in the co-pyrolysis process also was conducted, and the results are embedded in Fig. 5. For instance, when PE was employed, the theoretical value was calculated by the following equation:

where Y_{PC} and Y_{PE} are the peak areas of specific aromatic hydrocarbons obtained from catalytic fast pyrolysis of PC and PE, respectively. X_1 and X_2 are the mass percentages of PC and PE in total feedstocks.

As shown in Fig. 5, in the co-pyrolysis of PC with PS or PP trial, the experimental MAHs were higher than theoretical ones, indicating that there was a positive additive effect between the blended feedstocks which facilitated the generation of MAHs. Meanwhile, Fig. 7 presents the advanced factor of main MAHs attained from the co-pyrolysis of PC and PS over HZSM-5 (38). As observed, all the studied monocyclic aromatic targets were promoted as the advanced factors derived from the co-pyrolysis process were higher than those obtained from catalytic conversion of pure PC. For example, the advanced factor of styrene attained from co-pyrolysis reached 43.5, which corresponded to a 204.2 % yield increase over the catalytic degradation of PC only.

Regarding the formation of BAHs, the use of PE or PP to co-feed with PC reduced their production, while an opposite trend was observed upon employing PS as a hydrogen donor. For phenolic products, as expected, co-pyrolysis of PC with other hydrogen-rich plastics inhibited phenols formation as opposed to the catalytic conversion of pure PC, and the lowest content was attained in the PC co-fed with PP run. For instance, the relative content of phenols was 25.1 % in the catalytic degradation of pure PC, while it decreased to 6.3 %, 6.2 %, and 8.5 % when PS, PP, or PE was employed to co-pyrolyze with PC, respectively. In summary, since co-pyrolysis PC with PS not only maximized the MAHs with a high content of 76.6 % but also considerably inhibited the phenolic products, therefore, PS was selected as an optimal hydrogen donor to conduct the co-pyrolysis experiments.

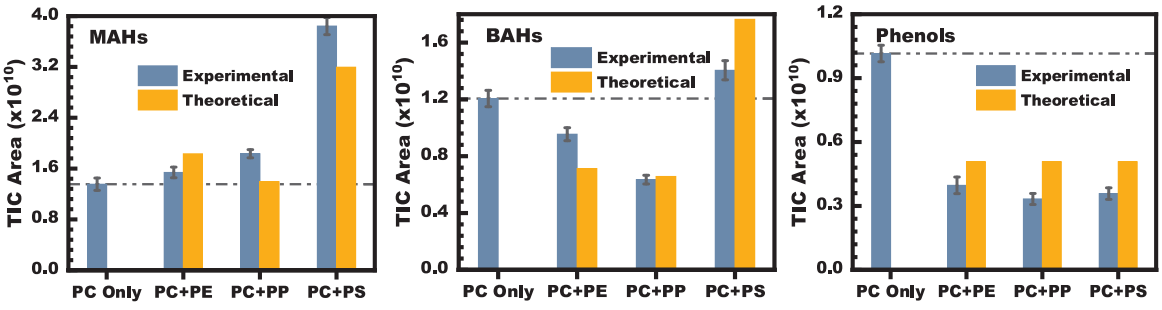
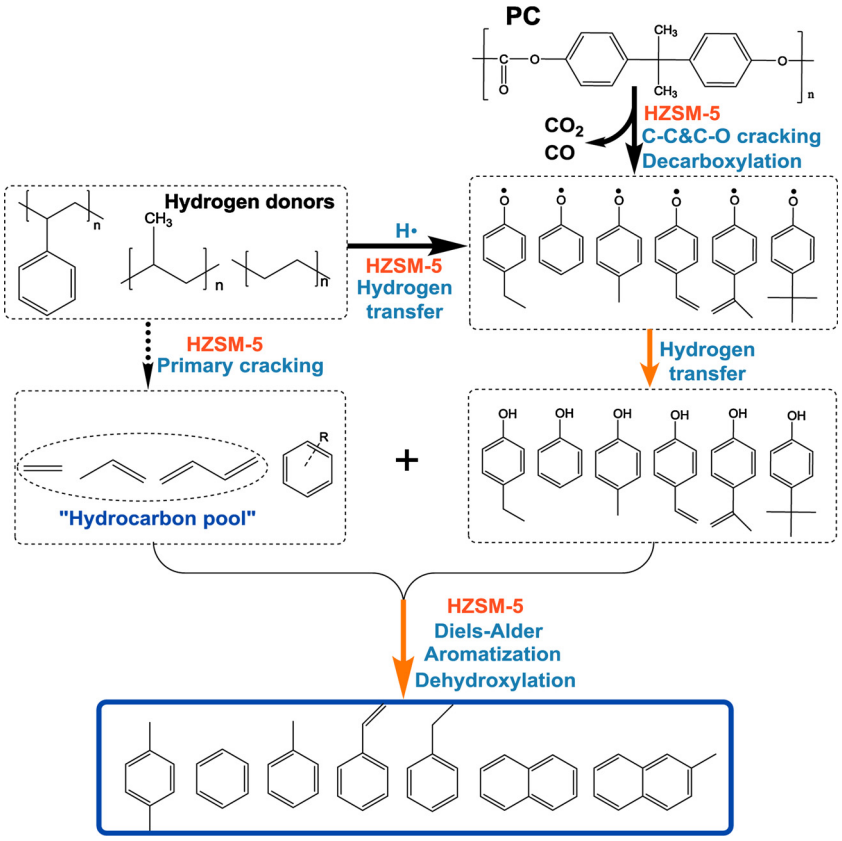


Fig. 5. Pyrolytic aromatic products obtained from catalytic fast co-pyrolysis of PC and hydrogen-rich plastic wastes.



Scheme 1. Proposed reaction pathway in the co-pyrolysis of PC with hydrogen-rich plastic wastes over HZSM-5 to produce aromatic hydrocarbons.

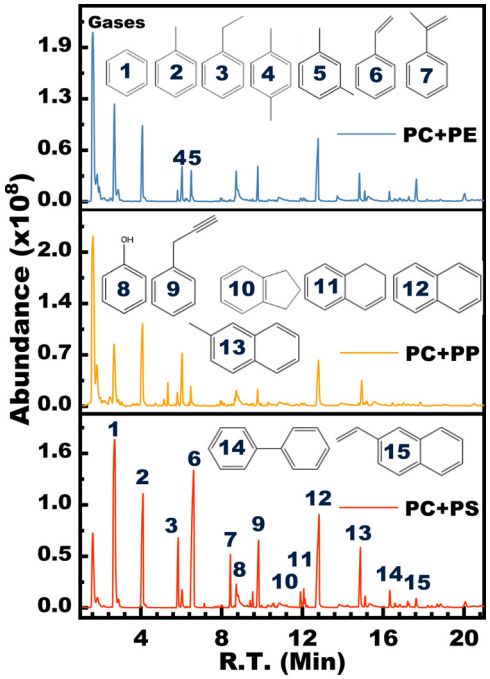


Fig. 6. GC/MS chromatograms derived from catalytic fast co-pyrolysis of PC with other plastic wastes over HZSM-5 (38).

3.4. Production of aromatic hydrocarbons as a function of PC percentage in the feedstock blends

To further study the effect of PC percentage in feedstock blends (i.e. varying H/C effective ratios) on the formation of aromatic hydrocarbons, experiments for co-pyrolysis of PC and PS over HZSM-5 with PC percentage ranging from 30 % to 90 % were conducted, and the pyrolytic products are illustrated in Fig. 8. Moreover, the additive effect (A_d, %) between PC and PS in the co-pyrolysis process also was calculated, shown as below:

$$A_d = \frac{Experimental - Theoretical}{Experimental} \times 100\%$$

As indicated, the content of total aromatic hydrocarbons gradually decreased with the increasing of PC percentage, while the additive

Table 1
The detailed distribution of MAHs obtained from catalytic conversion of pure PS, pure PC, and catalytic co-pyrolysis of PC and PS over HZSM-5 (38).

Chemical Name	Pure PC		PC + PS (1:1) [b]		Pure PS	
	R.T. [a]	Area (%)	R.T. [a]	Area (%)	R.T. [a]	Area (%)
MAHs (Total)		22.6		76.6		63.8
Benzene	2.7	10.8	2.7	26.3	2.7	18.7
Toluene	4.1	5.3	4.1	13.7	4.1	9.7
Ethylbenzene	5.8	0.3	5.9	5.4	5.9	3.9
p-Xylene	6.0	0.8	6.0	1.6	6.0	1.1
Styrene	6.5	1.8	6.6	21.3	6.7	21.3
Methyl-styrene	8.4	0.2	8.4	3.1	8.4	1.8
Benzene, 2-propenyl-	–	–	9.4	0.6	9.4	0.3
Benzene, 1-ethenyl-2-methyl-	–	–	9.5	0.8	8.7	0.3
Benzene, 1-propynyl-	9.8	2.9	10.0	0.2	9.5	0.9
Benzene, 1-ethenyl-3-ethyl-	–	–	10.6	0.5	10.6	0.5
1H-Indene, 1-methyl-	11.9	0.2	11.9	1.1	11.9	1.3
1H-Indene, 3-methyl-	12.1	0.2	12.1	1.1	12.1	1.3

[a] Retention time (Min).
[b] Mass ratio.

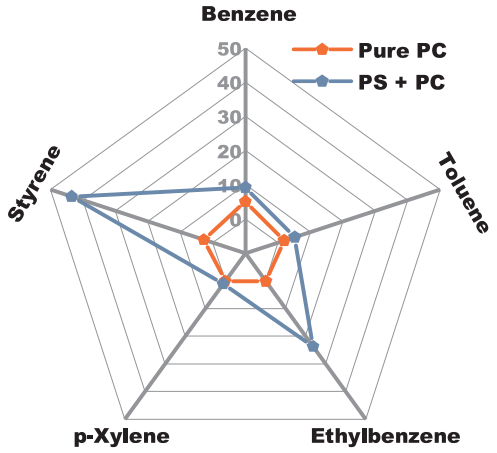


Fig. 7. The advanced factor of MAHs attained from catalytic conversion of pure PC and co-pyrolysis of PS and PC blends over HZSM-5 (38).

effect increased at first and then decreased with the highest value of 12.1 % obtained at 70 % PC. Additionally, the theoretical aromatic hydrocarbons were higher than the experimental ones when the PC percentage was elevated to 90 %, indicating a negative additive effect (-15.0 %) might occur which suppressed the production. Similarly, in the case of MAHs formed in the co-pyrolysis as a function of PC percentage, the content decreased when the PC percentage was increased from 30 % to 90 %. However, of particular note was that no negative additive effect for MAHs was observed within the studied full PC percentage range. Specifically, the additive effect increased from 5.6%–32.4% as the PC percentage elevated from 30 % to 70 %, and further elevating the percentage to 90 % dramatically lowered it to 5.9 %. Regarding the BAHs, as depicted in Fig. 8c, compared to the theoretical content, employing PS to co-feed with PC suppressed their formation as the additive effects were negative. Conversely, in the case of phenolic products, phenols gradually increased as the PC percentage was elevated from 30 % to 90 %, and negative additive effects (< -40 %) were observed when the percentage was below 50 %. However, higher PC proportion in feedstock blends was beneficial to form phenols as the additive effect increased to 41.6 % (at 70 %) and 37.7 % (at 90 %), respectively.

Fig. 9 depicts the distribution of MAHs, BAHs, and phenols obtained from the co-pyrolysis of PC and PS as a function of PC percentage. As described in Fig. 9a, the product distribution of MAHs was dominated by styrene at a low PC percentage of 30 %, and negligible xylene was produced under this condition. For benzene, the content increased when the PC percentage was elevated from 30 % to 50 %, however, further elevating the PC percentage to 70 % or 90 % inhibited its formation. In the case of ethylbenzene, 50 % and 70 % PC proportion produced comparable ethylbenzene, while a higher PC percentage declined its production.

Concerning the distribution of BAHs, as illustrated in Fig. 9b, the BAHs mainly were naphthalene and its derivates with naphthalene being the predominant. Naphthalene was slightly inhibited when the PC percentage increased from 30 % and 50 %, however, further increasing the PC percentage to 70 % resulted in a more significant decrease. Similarly, elevating the PC percentage from 30 % to 90 % also lowered methyl-naphthalene. In the case of dihydro-naphthalene, dimethyl-naphthalene, and ethyl-naphthalene (DDE), as shown, the generation of DDE was negligible with a low total content of ~1 %. More specifically, dihydro-naphthalene slightly fluctuated as the PC percentage increased from 30 % to 90 %, while elevating PC percentage inhibited the production of dimethyl-naphthalene and ethyl-naphthalene.

For phenolic products (mainly were phenol, cresols, and *p*-iso propenylphenol), as indicated in Fig. 9c, the distribution was dominated by phenol within the studied PC percentage range. For instance, the relative selectivity to phenol was 78.4 % and 56.9 % when the PC percentage was 30 % and 50 %, respectively (Fig. S3). Furthermore, elevating the PC percentage was beneficial to phenol as the content

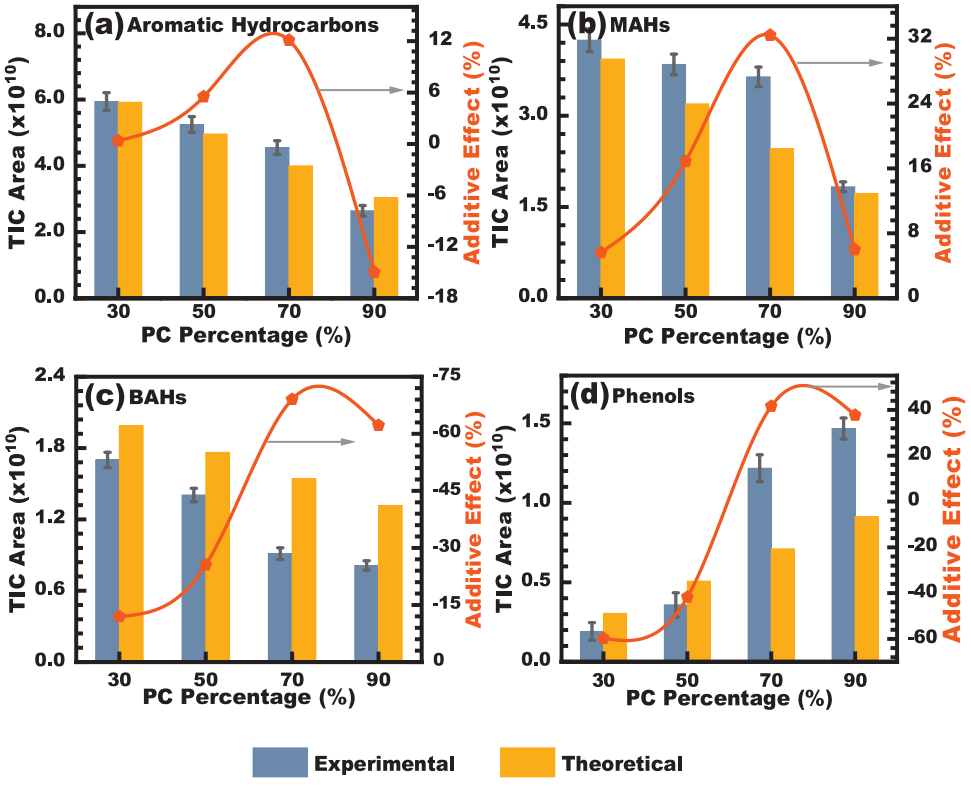


Fig. 8. Pyrolytic products derived from catalytic fast co-pyrolysis of PC and PS: Effect of PC percentage in feedstock blends.

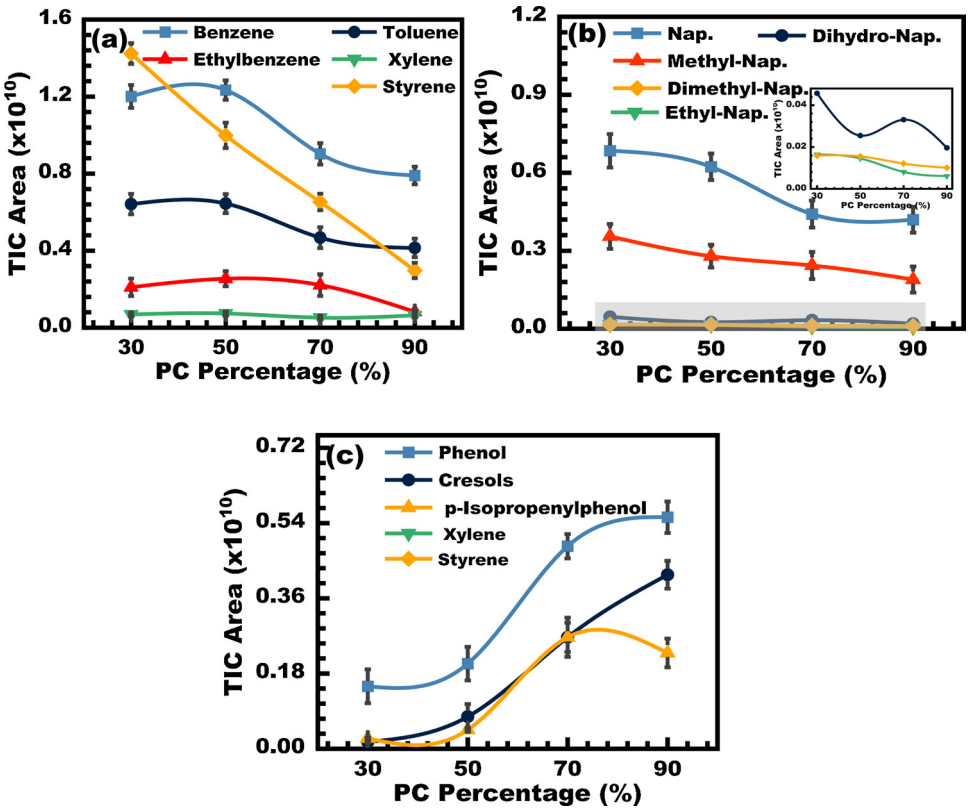


Fig. 9. The product distribution of aromatic hydrocarbons and phenols as a function of PC percentage in the catalytic fast co-pyrolysis of PC and PS over HZSM-5 (38).

increased gradually. Similarly, increasing PC percentage facilitated the relative selectivity of cresols as it increased from 8.5 % (for 30 % PC, Fig. S3) to 28.4 % at 90 % PC. For the production of *p*-isopropenylphenol, the content was increased when the PC percentage was elevated from 30 % to 70 %, while subsequently increasing the PC percentage to 90 % led to a contrary tendency.

4. Conclusions

Aromatic hydrocarbons were significantly facilitated in the HZSM-5 catalyzed run compared to those obtained non-catalytically, and a reaction temperature of 700 ˚C resulted in a ~5-fold increase. The distribution of MAHs was dominated by benzene and toluene in the catalytic conversion of pure PC over HZSM-5, and HZSM-5 (38) was more beneficial to form benzene with an advanced factor of 5.1 followed by HZSM-5 (25). Co-feeding PS with PC promoted all the studied monocyclic aromatic targets, and the additive factor of styrene attained from co-pyrolysis of PC and PS reached 43.5, indicating a 204.2 % increase in yield was attained in comparison to the catalytic degradation of pure PC. A positive additive effect of PC and PS for the production of MAHs was observed within the investigated PC percentage range, and a PC percentage of 70 % maximized the additive effect.

CRediT authorship contribution statement

Jia Wang: Conceptualization, Methodology, Writing - original draft, Visualization. **Jianchun Jiang:** Supervision, Funding acquisition. **Xiaobo Wang:** Methodology. **Ruizhen Wang:** Validation. **Kui Wang:** Funding acquisition. **Shusheng Pang:** Visualization. **Zhaoping Zhong:** Conceptualization. **Yunjuan Sun:** Funding acquisition. **Roger Ruan:** Conceptualization, Methodology. **Arthur J. Ragauskas:** Conceptualization, Writing - review & editing.

Declaration of Competing Interest

The authors declare that they have no known competing financial interests or personal relationships that could have appeared to influence the work reported in this paper.

Acknowledgments

The authors are grateful for the National Natural Science Foundation of China (No.31530010, 31870714), the Key Lab. of Biomass Energy and Material, Jiangsu Province (No. JSBEM-S-201602), the Natural Science Foundation of the Jiangsu Higher Education Institutions of China (No. 17KJB610005), the Talent Introduction Project Funded by National Forestry and Grassland Administration (No. KJZXSF2019002), and a project funded by Nanjing Xiaozhuang University (No.2016NXY41).

Appendix A. Supplementary data

Supplementary material related to this article can be found, in the online version, at doi:https://doi.org/10.1016/j.jhazmat.2019.121970.

References

Antonakou, E.V., Achilias, D.S., 2012. Recent advances in polycarbonate recycling: a review of degradation methods and their mechanisms. Waste Biomass Valoriz. 4, 9–21.

Antonakou, E.V., Kalogiannis, K.G., Stephanidis, S.D., Triantafyllidis, K.S., Lappas, A.A., Achilias, D.S., 2014a. Pyrolysis and catalytic pyrolysis as a recycling method of waste CDs originating from polycarbonate and HIPS. Waste Manag. 34, 2487–2493.

Antonakou, E.V., Kalogiannis, K.G., Stefanidis, S.D., Karakoulia, S.A., Triantafyllidis, K.S., Lappas, A.A., Achilias, D.S., 2014b. Catalytic and thermal pyrolysis of polycarbonate in a fixed-bed reactor: the effect of catalysts on products yields and composition. Polym. Degrad. Stab. 110, 482–491.

Bai, B., Jin, H., Fan, C., Cao, C., Wei, W., Cao, W., 2019. Experimental investigation on liquefaction of plastic waste to oil in supercritical water. Waste Manag. 89, 247–253.

Ben, H., Ragauskas, A.J., 2013. Influence of Si/Al ratio of ZSM-5 zeolite on the properties of lignin pyrolysis products. ACS Sustain. Chem. Eng. 1, 316–324.
Do, T., Baral, E.R., Kim, J.G., 2018. Chemical recycling of poly(bisphenol A carbonate): 1,5,7-Triazabicyclo[4.4.0]-dec-5-ene catalyzed alcoholysis for highly efficient bisphenol A and organic carbonate recovery. Polymer 143, 106–114.
Jae, J., Tompsett, G.A., Foster, A.J., Hammond, K.D., Auerbach, S.M., Lobo, R.F., Huber, G.W., 2011. Investigation into the shape selectivity of zeolite catalysts for biomass conversion. J. Catal. 279, 257–268.
Kassargy, C., Awad, S., Burnens, G., Upreti, G., Kahine, K., Tazerout, M., 2019. Study of the effects of regeneration of USY zeolite on the catalytic cracking of polyethylene. Appl. Catal. B 244, 704–708.
Mehmood, M.A., Ahmad, M.S., Liu, Q., Liu, C.-G., Tahir, M.H., Aloqbi, A.A., Tarbiah, N.I., Alsufiani, H.M., Gull, M., 2019. Helianthus tuberosus as a promising feedstock for bioenergy and chemicals appraised through pyrolysis, kinetics, and TG-FTIR-MS based study. Energy Convers. Manage. 194, 37–45.
Mullen, C.A., Boateng, A.A., 2010. Catalytic pyrolysis-GC/MS of lignin from several sources. Fuel Process. Technol. 91, 1446–1458.
Park, Y.-K., Jung, J.S., Jae, J., Hong, S.B., Watanabe, A., Kim, Y.-M., 2018. Catalytic fast pyrolysis of wood plastic composite over microporous zeolites. Chem. Eng. J.
Park, Y.K., Han, T.U., Jeong, J., Kim, Y.M., 2019a. Debrominated high quality oil production by the two-step catalytic pyrolysis of phenolic printed circuit boards (PPCB) using natural clays and HY. J. Hazard. Mater. 367, 50–58.
Park, Y.-K., Lee, B., Lee, H.W., Watanabe, A., Jae, J., Tsang, Y.F., Kim, Y.-M., 2019b. Co-feeding effect of waste plastic films on the catalytic pyrolysis of Quercus variabilis over microporous HZSM-5 and HY catalysts. Chem. Eng. J. 378.
Rezaei, P.S., Oh, D., Hong, Y., Kim, Y.-M., Jae, J., Jung, S.-C., Jeon, J.-K., Park, Y.-K., 2017. In-situ catalytic co-pyrolysis of yellow poplar and high-density polyethylene over mesoporous catalysts. Energy Convers. Manage. 151, 116–122.
Ryu, H.W., Tsang, Y.F., Lee, H.W., Jae, J., Jung, S.-C., Lam, S.S., Park, E.D., Park, Y.-K., 2019. Catalytic co-pyrolysis of cellulose and linear low-density polyethylene over MgO-impregnated catalysts with different acid-base properties. Chem. Eng. J. 373, 375–381.
Sebestyén, Z., Barta-Rajnai, E., Bozi, J., Blazsó, M., Jakab, E., Miskolczi, N., Sója, J., Czégény, Z., 2017. Thermo-catalytic pyrolysis of biomass and plastic mixtures using HZSM-5. Appl. Energy 207, 114–122.
Shahid, A., Ishfaq, M., Ahmad, M.S., Malik, S., Farooq, M., Hui, Z., Batawi, A.H., Shafi, M.E., Aloqbi, A.A., Gull, M., Mehmood, M.A., 2019. Bioenergy potential of the residual microalgal biomass produced in city wastewater assessed through pyrolysis, kinetics and thermodynamics study to design algal biorefinery. Bioresour. Technol. 289, 121701.
Tang, H., Hu, Y., Li, G., Wang, A., Xu, G., Yu, C., Wang, X., Zhang, T., Li, N., 2019. Synthesis of jet fuel range high-density polycycloalkanes with polycarbonate waste. Green Chem. 21, 3789–3795.
Wang, J., Jiang, J., Zhong, Z., Wang, K., Wang, X., Zhang, B., Ruan, R., Li, M., Ragauskas, A.J., 2019. Catalytic fast co-pyrolysis of bamboo sawdust and waste plastics for enhanced aromatic hydrocarbons production using synthesized CeO2/γ-Al2O3 and HZSM-5. Energy Convers. Manage. 196, 759–767.
Xue, Y., Bai, X., 2018. Synergistic enhancement of product quality through fast co-pyrolysis of acid pretreated biomass and waste plastic. Energy Convers. Manage. 164, 629–638.
Yao, D., Yang, H., Chen, H., Williams, P.T., 2018a. Investigation of nickel-impregnated zeolite catalysts for hydrogen/syngas production from the catalytic reforming of waste polyethylene. Appl. Catal. B 227, 477–487.
Yao, D., Yang, H., Chen, H., Williams, P.T., 2018b. Co-precipitation, impregnation and sol-gel preparation of Ni catalysts for pyrolysis-catalytic steam reforming of waste plastics. Appl. Catal. B 239, 565–577.
Yu, D., Hui, H., Li, S., 2019. Two-step catalytic co-pyrolysis of walnut shell and LDPE for aromatic-rich oil. Energy Convers. Manage. 198.
Zhang, H., Likun, P.K.W., Xiao, R., 2018. Improving the hydrocarbon production via co-pyrolysis of bagasse with bio-plastic and dual-catalysts layout. Sci. Total Environ. 618, 151–156.
Zhang, H., Cheng, Y.-T., Vispute, T.P., Xiao, R., Huber, G.W., 2011. Catalytic conversion of biomass-derived feedstocks into olefins and aromatics with ZSM-5: the hydrogen to carbon effective ratio. Energy Environ. Sci. 4, 2297.
Zhang, X., Lei, H., Zhu, L., Qian, M., Zhu, X., Wu, J., Chen, S., 2016. Enhancement of jet fuel range alkanes from co-feeding of lignocellulosic biomass with plastics via tandem catalytic conversions. Appl. Energy 173, 418–430.
Zhang, Z., Gora-Marek, K., Watson, J.S., Tian, J., Ryder, M.R., Tarach, K.A., López-Pérez, L., Martínez-Triguero, J., Melián-Cabrera, I., 2019a. Recovering waste plastics using shape-selective nano-scale reactors as catalysts. Nat. Sustain. 2, 39–42.
Zhang, H., Shao, S., Luo, M., Xiao, R., 2017a. The comparison of chemical liquid deposition and acid dealumination modified ZSM-5 for catalytic pyrolysis of pinewood using pyrolysis-gas chromatography/mass spectrometry. Bioresour. Technol. 244, 726–732.
Zhang, C., Kwak, G., Park, H.-G., Jun, K.-W., Lee, Y.-J., Kang, S.C., Kim, S., 2019b. Light hydrocarbons to BTEX aromatics over hierarchical HZSM-5: effects of alkali treatment on catalytic performance. Microporous Mesoporous Mater. 276, 292–301.
Zhang, H., Ma, Y., Shao, S., Xiao, R., 2017b. The effects of potassium on distributions of bio-oils obtained from fast pyrolysis of agricultural and forest biomass in a fluidized bed. Appl. Energy 208, 867–877.
Zhang, Y., Duan, D., Lei, H., Villota, E., Ruan, R., 2019c. Jet fuel production from waste plastics via catalytic pyrolysis with activated carbons. Appl. Energy 251.